Distributed-element Preisach model for hysteresis of shape memory alloys

C Song, J A Brandon and C A Featherston

The online version of this article can be found at:

http://pic.sagepub.com/content/215/6/673

Published by:

$SAGE

http://www.sagepublications.com

On behalf of:

Institution of MECHANICAL ENGINEERS

Institution of Mechanical Engineers

Additional services and information for *Proceedings of the Institution of Mechanical Engineers, Part C: Journal of Mechanical Engineering Science* can be found at:

Email Alerts: http://pic.sagepub.com/cgi/alerts

Subscriptions: http://pic.sagepub.com/subscriptions

Reprints: http://www.sagepub.com/journalsReprints.nav

Permissions: http://www.sagepub.com/journalsPermissions.nav

Citations: http://pic.sagepub.com/content/215/6/673.refs.html

>> Version of Record - Jun 1, 2001

What is This?

Distributed-element Preisach model for hysteresis of shape memory alloys

C Song, J A Brandon* and **C A Featherston**
Mechanical Engineering and Energy Studies Division, Cardiff School of Engineering, Cardiff University, Wales, UK

Abstract: The paper describes the development of distributed-element models for non-linear hysteresis in materials and structures. The physical model is based on an approach that views the system as comprising a series of ideal elastoplastic elements. Parameter identification, numerical simulation and inversion of the model through the application of the Preisach model for hysteresis are discussed. Experimentally obtained data using Nitinol are compared with the model prediction, thus establishing the effectiveness of distributed-element Preisach elements for predicting complex hysteresis effects including high-order hysteresis transition curves.

Keywords: shape memory alloys, hysteresis, non-linear modelling

NOTATION

f	system output
F	function defined in equation (18)
P	play operator
R	relay operator
S	stop operator
u	system input
α	operator switch value
β	operator switch value
ε	stress
μ	weight function
σ	strain

1 INTRODUCTION

Hysteresis phenomena are present in many physical systems. These range from systems comprising a single element, such as shape memory alloys (SMAs), piezoceramics, electrorheology (ER) and magnetorheology (MR), where material damping may be significant, to structures consisting of a number of separate elements. In the latter case, the hysteresis of the system can result from the behaviour of one or more elements (for example, the plastic yielding of some portion of a structure) or from such mechanisms as slip between different elements of the system.

From the physical point of view, hysteresis can be a byproduct of fundamental mechanisms (such as phase transitions in SMAs and domain wall motion in ferromagnetic materials) or a consequence of a degradation or imperfection, or built deliberately into a system in order to monitor its behaviour, as in the case of heat control via thermostats.

There is a need either to develop new models or to exploit existing theory to represent the underlying physical process while attaining compatibility with design representations. In the current paper the operator models devised by Preisach [1] in the 1930s, for magnetic materials, are demonstrated to apply to the bulk properties of the most common SMA. The resulting stress–strain map is consistent with the use of local modification theory in otherwise linear models [2, 3].

Hysteresis is a genuinely non-linear phenomenon that is not straightforward to treat mathematically. A variety of mathematical models for hysteresis have been developed. Among these, the Preisach model plays a key role owing to its clear definition and simple identification. The Preisach model can be tracked back to the landmark paper published by Preisach in 1935 [1]. It was first regarded as a physical model of hysteresis, but it was subsequently realized that it is more phenomenological in nature. In the 1970s and 1980s, the mathematical properties of the Preisach model were developed by Russian mathematicians Krasnoselskii and Pokrovskii [4], who abstracted the model and represented it in a purely mathematical form similar to a spectral

decomposition of operators. Significant recent contributions to the general theory of hysteresis operators can also be found in references [5] to [7]. The Preisach model has several attractive features including its ability to model complex hysteresis types, a well-defined identification algorithm and a convenient numerical simulation method. It has been used successfully for modelling various types of hysteresis.

As will be demonstrated, the pseudoelastic hysteresis with non-local memory exhibited by SMAs can be modelled by the Preisach model. A form of the Preisach model with four parameters was applied to represent individual SMA crystals by Huo [8]. The model predictions were consistent with experimental data [8]. The control parameter was stress and the observed parameter was strain; all the experiments were performed at constant temperatures. A standard Preisach model was applied to a single large crystal of CuZnAl by Ortin [9] with a satisfactory correlation between the model and experiment. Hughes and Wen [10] applied the Preisach model for the hysteresis of piezoceramic and shape memory materials, with complex hysteresis effects such as minor loop congruency and wiping-out (q.v.) modelled successfully.

Originally, the Preisach model was based on hypotheses concerning the physical mechanism of magnetization. For this reason, it was first regarded as a restricted physical model of hysteresis. However, in the applications mentioned above, the Preisach modelling of SMA hysteresis was a much more abstract model where the identified parameters in the Preisach model lack physical meaning. For this reason, the current paper applies the distributed-element model for hysteresis and redefines the elementary hysteresis operators, relating them to the observed properties of SMAs. A hysteresis model with concise mathematical expression and clear physical explanation is then formulated.

The distributed-element model for hysteresis in mechanical systems has been researched by Iwan [11–13] and by Cifuentes and Iwan [14]. It was based on the assumption that a general hysteretic system may be thought of as comprising a large number of ideal elastoplastic elements with different yield levels. This approach was suggested by Timoshenko [15] as early as 1930 but had subsequently received little attention. The most likely reason for this is that the idea of a distributed-element system is somewhat oversimplified [16] and the feeling that a distributed-element approach might lead to complex formulation of the force–deflection relations. This, however, is not the case. The intention of the present paper is to show that the distributed-element formulation can be used to generate a relatively simple hysteretic model that exhibits the essential features of complex hysteresis phenomena and can be readily applied to investigate a hysteretic system by using the mathematical advantages of the Preisach model.

2 HYSTERESIS OPERATORS

Hysteresis operators play a key role in the mathematical study of hysteretic phenomena. A hysteresis operator maps an input function $u = u(t)$ into a corresponding output function $f = f(t)$, where t represents the time variable. Using this formulation, the paper illustrates the structures and the memory effects of various basic hysteresis models. The relevant connections between the different types of hysteresis operator are established. The approach via hysteresis operators originates from the Krasnoselskii and Pokrovskii school [4] (see also references [5] and [6]).

2.1 Relay operator

The simplest example of a hysteresis non-linearity is given by a relay operator, as shown in Fig. 1. The relay is characterized by two switch values, α and β, and two output values, which, without loss of generality, are assumed to be equal to $+1$ and -1 respectively; alternatively, the mean value $s = (\alpha + \beta)/2$ and the half-width $r = (\alpha - \beta)/2$ may be used. The input–output relation behaviour described by Fig. 1 can be expressed by an operator of the form

$$f = \mathbf{R}_{\alpha,\beta}[u] \tag{1}$$

where $\mathbf{R}_{\alpha,\beta}$ is the relay operator with switch values $\beta < \alpha$.

2.2 Play operator

A slightly more complex example of non-linearity is given by the mechanical play operator which has two elements. The play is modelled as a combination of a
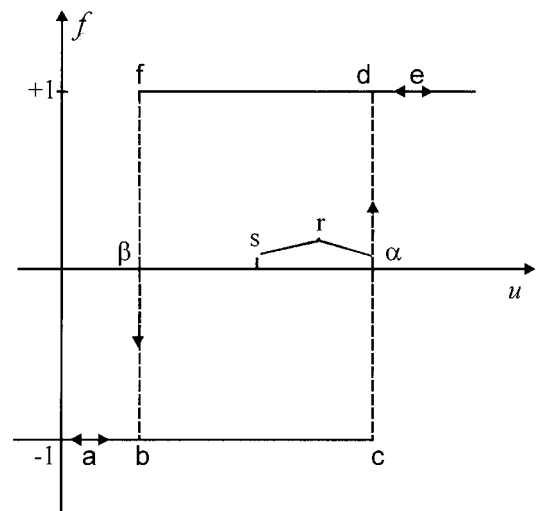

Fig. 1 Relay with hysteresis

linear spring with stiffness k and a Coulomb or slip damper which has a maximum allowable yield force r. If force f is regarded as the input, and displacement u as the output, the corresponding input–output relation is given by the hysteresis diagram in Fig. 2b. In operator form, for $r \geqslant 0$,

$$f = P_r[u] \tag{2}$$

where P_r is the operator of *scalar mechanical play* or simply the *play operator*. The play operator can be expressed as a linear superposition of relay elements:

$$P_r[u](t) = \tfrac{1}{2} \int_{-\infty}^{+\infty} R_{s-r,s+r}[u](t) \, ds \tag{3}$$

2.3 Stop operator

Another basic hysteresis non-linearity is given by the force–displacement (stress–strain) relation in a one-dimensional elastoplastic element (Fig. 3a). Once the output force has reached the yield value, it remains constant with further increases in the displacement. Elastic behaviour, however, is recovered when the displacement is lowered again. Here

$$f = S_r[u] \tag{4}$$

where S_r is the *stop operator* or *elastoplastic operator*.

The operators P_r and S_r are closely related through the following equation:
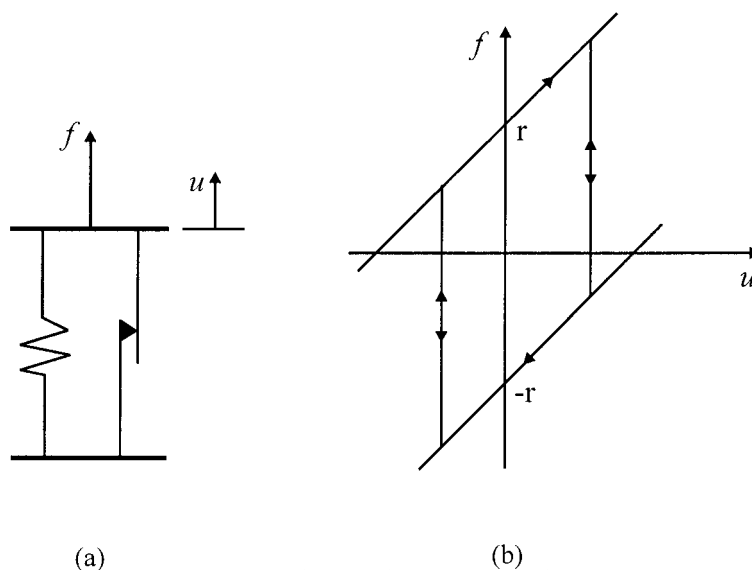
$$P_r + S_r = Id \tag{5}$$

(a)   (b)

Fig. 2 Hysteresis behaviour of mechanical play
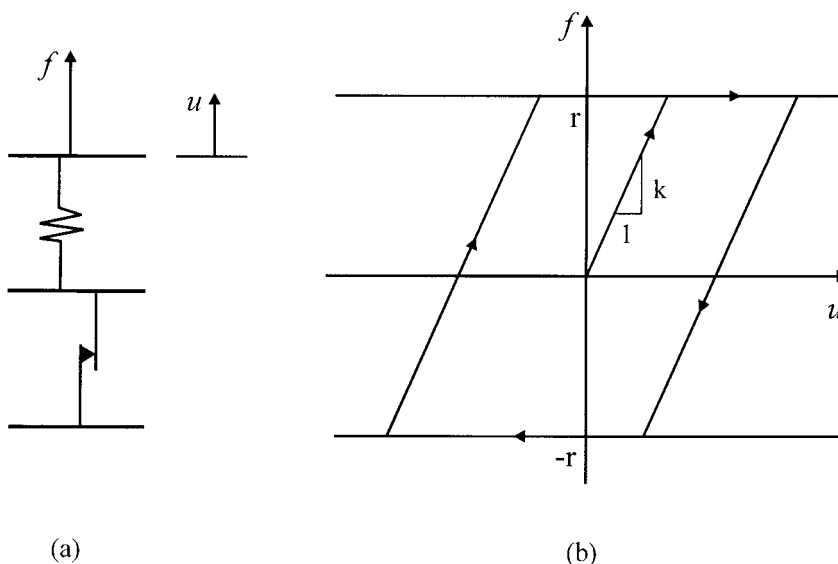

(a)   (b)

Fig. 3 Hysteresis behaviour of the stop operator

Id is the identity operator. This means that, for the monotone input during $t \in [t_i, t_{i+1}]$, the output is

$$f = f[u] = P_r[u] + S_r[u] = \text{Id}[u] = u \tag{6}$$

Through equations (5) and (6), it can be seen that the stop operator can also be expressed as a linear superposition of the basic relay operators.

3 SMA HYSTERESIS

Strong hysteretic effects have been found in all SMAs, including NiTi and Cu-based alloys. From a macroscopic point of view, there are two primary hysteretic properties of SMAs: the shape memory effect (SME) and pseudoelasticity (PE), which is the concern of this paper.

Hysteresis in SMAs is strongly influenced by temperature. When an SMA is at high temperature (specifically exceeding the austenite finish temperature, A_f) a large inelastic strain due to stress-induced austenite to martensite transformation will occur after linear elastic deformation, but this strain recovers completely through hysteresis on unloading by the reverse transformation shown in Fig. 4. When the yield load is exceeded (Fig. 4b), the austenite variant transforms into martensitic twins, accompanied with a large strain (Fig. 4c). On unloading, the austenite phase is re-established, and the original shape is recovered (Fig. 4d). The reason for this full recovery of the inelastic strain is that the stress-induced martensites are unstable in the absence of stress at temperatures above A_f, so that the reverse transformation to stable austenite occurs upon unloading [17].

The hysteresis of SMA shows two remarkable features:

1. The hysteresis is static, i.e. within some limits it is independent of the variation rate of the parameter controlling the transformation (temperature or stress).

2. The hysteresis exhibits global memory (as opposed to local memory), i.e. the transformed volume for a given value of temperature or stress can only be determined from the path that has been followed in the T–σ–ε space.

The hysteretic shapes of SMA can be affected significantly by several factors, such as temperature and strain rate, loading history and some comparatively complicated fatigue effects. A number of hysteretic models have been developed on the basis of thermodynamic considerations, micromechanics or phenomenology [18–20].

The effects of elastic strain energy and frictional force are the controlling factors for the generation of transformation hysteresis. The release of frictional energy creates an energy loss. The greater the frictional energy, the broader the hysteresis. The elastic energy that is stored or released during transformation will hinder the forward transformation but will assist the reverse transformation [21].

Based on the analysis above, and the hysteresis behaviour shown in Fig. 4, the SMA crystal can be modelled as a stack of layers parallel to the habit plane, the plane whose direction will not change during phase transformation where only shear strain is allowed in that plane. Because no volume change occurs during the transformation, it can be assumed that the displacement, d, in that direction depends only on the x coordinate which is perpendicular to the habit plane (i.e. x runs in the stacking direction), as well as on the time, t. The model is shown in Fig. 5.

With the displacement $d(x, t)$, the local shear strain $\varepsilon(x, t)$ is defined by

$$\varepsilon(x, t) = \frac{\partial d}{\partial x}(x, t) = d_x(x, t) \tag{7}$$

while the velocity in the shear direction is given by

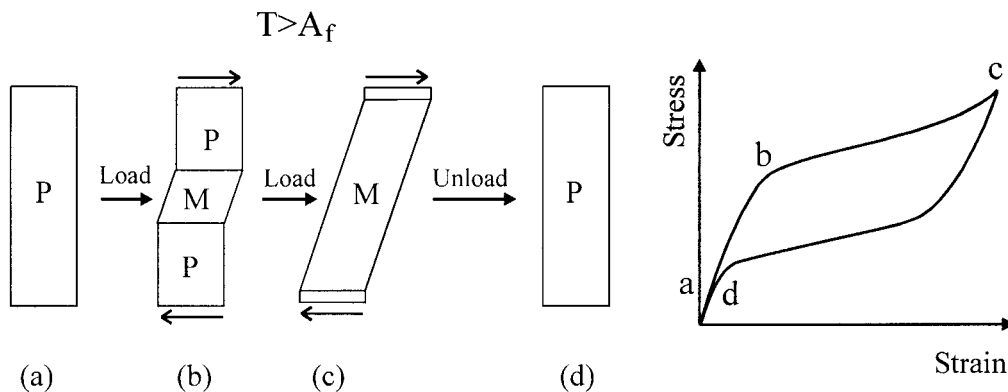$$v(x, t) = \frac{\partial d}{\partial t}(x, t) = d_t(x, t) \tag{8}$$

Fig. 4 Schematic illustration of the mechanism of hysteresis in an SMA: P for parent phase; M for martensite
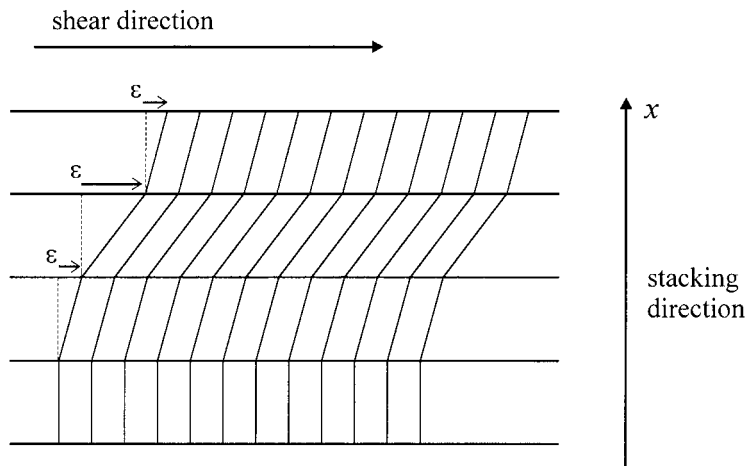
shear direction

Fig. 5 One-dimensional model for SMAs

4 DISTRIBUTED-ELEMENT MODEL

Based on the defined hysteresis operators and the analysis for SMA, a distributed-element model for the hysteresis of SMA, regarded as a system comprising a series of basic hysteresis elements, can now be developed. Taking stress as the input $u(t)$ and strain as the output $f(t)$, the model for an SMA shown in Fig. 5 can be regarded as a series of plays as indicated in Fig. 6a.

If the stress–strain relation for the entire system in Fig. 6a is now considered, it can be seen that the total strain of the system is made up of contributions from those elements that have already yielded. Without loss of generality, it can be assumed that the elements are arranged in order of increasing yield force r_i. Thus, the total strain upon loading will be

$$f(t) = \sum_{i=1}^{n} P_{r_i}[u(t)] \tag{9}$$

where n is the number of elements in a yielded state.

By using equation (3), the following may be obtained:

$$f(t) = \sum_{i=1}^{n} \frac{1}{2} \int_{-\infty}^{+\infty} R_{s-r_i, s+r_i}[u(t)] \, \mathrm{d}s \tag{10}$$

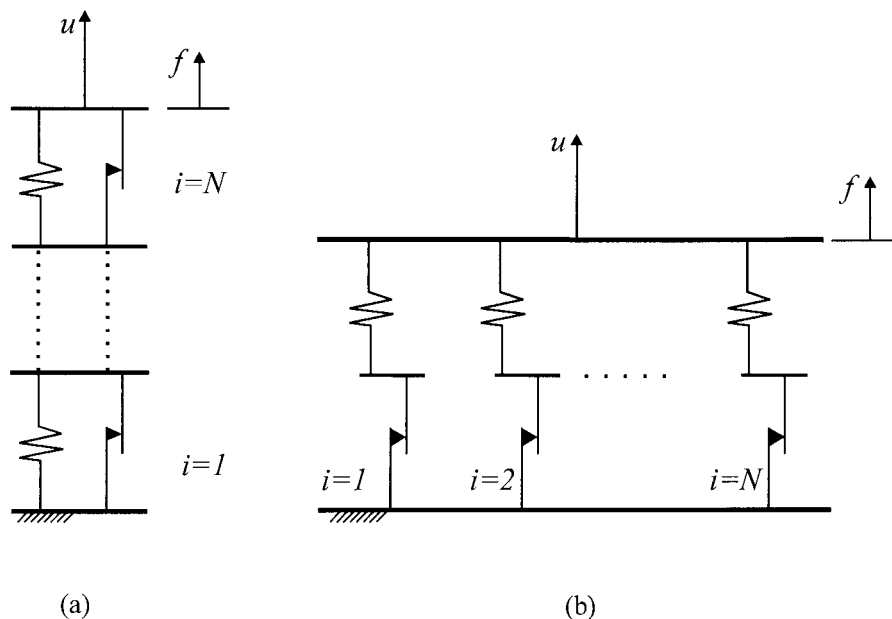(a)   (b)

Fig. 6 (a) Distributed-element model with stress as input and strain as output and (b) the inverse model with strain as input and stress as output

If the total number of elements, N, becomes infinite, the yield force will increase to infinity, and equation (10) then becomes

$$f(t) = \int_0^{+\infty} \tfrac{1}{2} \, dr \int_{-\infty}^{+\infty} R_{s-r,s+r}[u(t)] \, ds \qquad (11)$$

Actually the r and s are limited values, since $s = (\alpha + \beta)/2$ and $r = (\alpha - \beta)/2$ as shown in Fig. 1. To aid understanding and identification of relays, equation (11) can be rewritten in terms of α and β:

$$f(t) = \hat{\Gamma}[u(t)] = \iint_{\alpha \geqslant \beta} \mu(\alpha, \beta) R_{\alpha\beta}[u(t)] \, d\alpha \, d\beta \qquad (12)$$

Equation (12) for hysteresis defines the Preisach model. Here $\hat{\Gamma}$ is used for the concise notation of the Preisach hysteresis operator which is defined by the integral in equation (12) and $\mu(\alpha, \beta)$ is a weight function with a support area $\alpha \geqslant \beta$. Since $\alpha, \beta(\leqslant M)$ are limited values, it is assumed that $\mu(\alpha, \beta)$ is zero for α, β larger than M.

4.1 Main properties of the model

Now it can clearly be seen that, for modelling the hysteresis of SMAs, the Preisach model is physically based. If all the parameters (that is, r_i, k_i) of the mechanical plays shown in Fig. 6a can be identified through input/output experiments, the output $f(t)$ can be predicted from equation (11). Actually, from equation (12) it can be seen that the output of the Preisach model is the integral of function $\mu(\alpha, \beta) R_{\alpha\beta}$, and the outputs of $R_{\alpha\beta}$ are 1 and -1 only. Therefore, once the weight function $\mu(\alpha, \beta)$ is identified, the output of the system can be calculated through equation (12).

It follows that, at any instant t, the Preisach plane S may be divided into two areas, S^+ where the relay outputs are $+1$, and S^- where relay outputs are -1. They are illustrated in Fig. 7 which shows the geometric interpretation of the Preisach model. The two areas are separated by a staircase interface. The vertices of the staircase are determined by the previous reversal points of the inputs.

At any instant of time, therefore, the integral in (12) can be subdivided into two integrals, over $S^+(t)$ and $S^-(t)$, respectively:

$$f(t) = \hat{\Gamma}[u(t)]$$
$$= \iint_{S^+(t)} \mu(\alpha, \beta) \, d\alpha \, d\beta + \iint_{S^-(t)} \mu(\alpha, \beta) \, d\alpha \, d\beta \qquad (13)$$
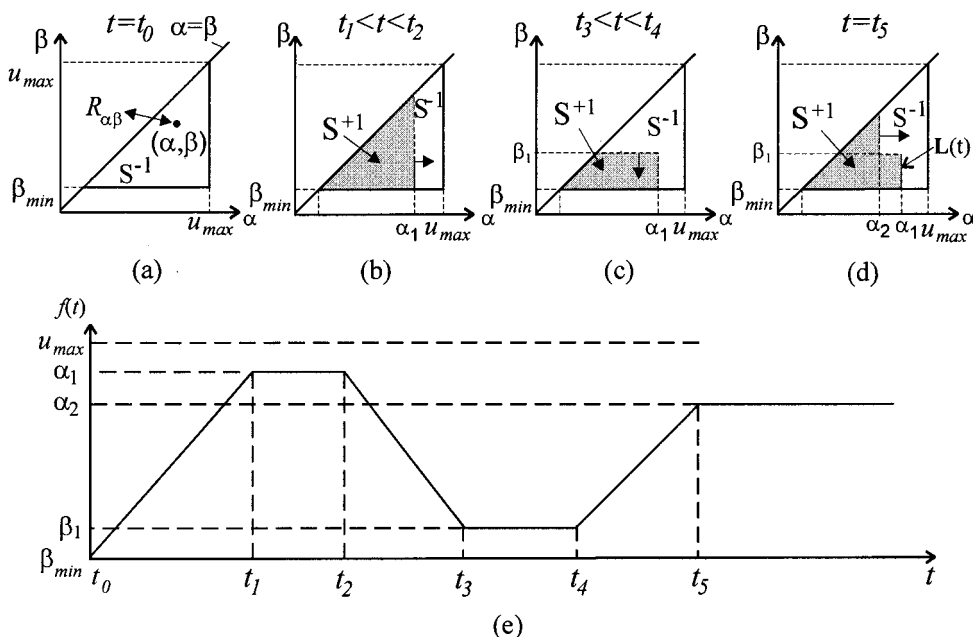
since

$$R_{\alpha\beta}[u(t)] = +1 \qquad \text{if } (\alpha, \beta) \in S^+(t) \qquad (14)$$

and

$$R_{\alpha\beta}[u(t)] = -1 \qquad \text{if } (\alpha, \beta) \in S^-(t) \qquad (15)$$

The geometric interpretation explains how the output is affected by the integration support area S which is

Fig. 7 Geometric interpretation of the model

changed by the input extrema. Not all the input extrema are remembered by the model. The input maximum wipes out the vertices whose α coordinates are below this input, and each input minimum wipes out the vertices whose β are above this minimum. This is called the *wiping-out property* of the model.

As the input increases, a vertical line of $\sigma(t)$ moves in the positive α direction in S, changing all the relay outputs to the left of the line to the $+1$ state. As the input decreases, a horizontal line moves in the negative β direction in S, changing all the relay outputs above the line to the -1 state.

At the starting point $t = 0$, the input $u(t)$ is at minimum β_{min} and all the relay outputs are in -1 (Fig. 7a). As the input increases to α_1 at t_1, a vertical line moves to α_1 from β_{min}, and the outputs of the relays on the left side of the line switch to $+1$ (Fig. 7b). From t_2 to t_3, the input is lowered to β_1, and a horizontal line sweeps down to β_1, changing some of the relay outputs back to -1 (Fig. 7c). When the input is increased again to α_2, some relays are changed to $+1$ (Fig. 7d). The output $f(t)$ at each time t is simply the integral of $\mu(\alpha, \beta)$ weighted by the corresponding relay outputs. It depends on the final staircase interfaces between S$^+$ and S$^-$. A constant input $u(t)$ will keep the output $f(t)$ constant.

Another characteristic property of the Preisach model is called the *congruency property*. If the input varies within the same range, from Fig. 7 it can be seen that the final link of the staircase interfaces will move identically within the same triangles. If the input goes monotonically from u_1 to u_2 and then back to u_1, the change in the relay output is the same irrespective of the initial conditions. The only effect of the initial condition is to produce a shift in the output. These two properties constitute the necessary and sufficient conditions for a non-linear hysteresis to be represented by the Preisach model for a set of piecewise monotonic inputs [5].

4.2 Identification of $\mu(\alpha, \beta)$

The weight function $\mu(\alpha, \beta)$ can be identified from a set of experimental first-order transition curves. The term 'first order' is used to emphasize the fact that each of these curves is formed from the first reversal of input. Figure 8 shows the use of first-order reversal curves for identification of the weight function $\mu(\alpha, \beta)$. From the geometric interpretation it is clear that f_α and $f_{\alpha\beta}$ can be written as

$$f_\alpha = \iint\limits_{S^+ + T} \mu(\alpha, \beta)\, \mathrm{d}a\, \mathrm{d}b + \iint\limits_{S^-} \mu(\alpha, \beta)\, \mathrm{d}a\, \mathrm{d}b \qquad (16)$$

$$f_{\alpha\beta} = \iint\limits_{S^+} \mu(\alpha, \beta)\, \mathrm{d}a\, \mathrm{d}b + \iint\limits_{S^- + T} \mu(\alpha, \beta)\, \mathrm{d}a\, \mathrm{d}b \qquad (17)$$

Now it is possible to define the function

$$\mathrm{F}(\alpha, \beta) \equiv \tfrac{1}{2}\left(f_\alpha - f_{\alpha\beta}\right) \qquad (18)$$

From equations (16) to (18) it can be established that

$$\mathrm{F}(\alpha, \beta) = \iint\limits_{\alpha \geqslant a \geqslant b \geqslant \beta} \mu(a, b)\, \mathrm{d}a\, \mathrm{d}b$$

$$= \int_\beta^\alpha \mathrm{d}a \int_\beta^a \mu(a, b)\, \mathrm{d}b \qquad (19)$$

Differentiating equation (19) twice yields

$$\mu(\alpha, \beta) = -\frac{\partial^2 \mathrm{F}(\alpha, \beta)}{\partial \alpha\, \partial \beta} \qquad (20)$$

Hence, the weight function $\mu(\alpha, \beta)$ can be calculated from $\mathrm{F}(\alpha, \beta)$, which in turn can be obtained from the set of experimental first-order transition curves. This makes the Preisach model particularly attractive. It not only reproduces the local memory features of partial hysteresis loops but also is able to predict the higher-order transition curves (i.e with multiple loops within the envelope) using a limited set of first-order experimental data.
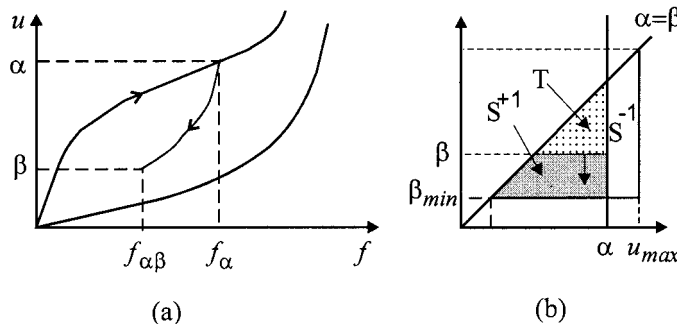
Fig. 8 (a) f_α and $f_{\alpha\beta}$ from first-order reversal and (b) the support of integration associated with $\mathrm{F}(\alpha, \beta)$

4.3 Numerical simulation

The Preisach model can be numerically implemented by using equation (12) for the computation of output $u(t)$ and equation (20) for the identification of the weight function $\mu(\alpha, \beta)$. However, the use of this approach creates two difficulties:

1. It requires the numerical evaluation of the double integral in equation (12), which is time consuming.
2. The identification of the weight function requires differentiation of experimental data, which may strongly amplify noise.

However, another approach can be developed for the numerical implementation of the Preisach model.

For an input history, a set of dominant maxima and minima can be determined. The relay outputs are then determined by the support area S. It is easy to see that the output of the Preisach model can be expressed as follows:

For an ascending branch

$$
f(t) = f_{\min} + \sum_{i=1}^{n(t)-1} \left(f_{\alpha_i \beta_i} - f_{\alpha_i \beta_{i-1}} \right)
$$
$$
+ \left(f_{u(t)} - f_{u(t)\beta_{N-1}} \right) \tag{21}
$$

For a descending branch

$$
f(t) = f_{\min} + \sum_{i=1}^{n(t)-1} \left(f_{\alpha_i \beta_i} - f_{\alpha_i \beta_{i-1}} \right)
$$
$$
+ \left(f_{\alpha_N u(t)} - f_{\alpha_N \beta_{N-1}} \right) \tag{22}
$$

where $f_{\min}$ is the output corresponding to the starting point $u_{\min}$, when all relay outputs are -1, and N is the number of input extrema.

Equations (21) and (22) can be used for direct calculation of the output based only on $F(\alpha, \beta)$ and not $\mu(\alpha, \beta)$. These expressions constitute the basis for the numerical implementation of the Preisach model. Detailed derivations can be found in reference [5]. This procedure avoids the important uncertainties associated with a double derivative of function $F(\alpha, \beta)$, affected by experimental noise, and the time-consuming double integral in equation (12).

4.4 Inverse problem

The inverse Preisach model is clearly physically represented (Fig. 6b) by the parallel distributed-element hysteresis model. With the same experimental data, the numerical inverse of the Preisach model can be easily derived from (21) and (22) if the first-order output $f(t)$ curves are strictly monotonic with the input $u(t)$. This has been observed to be the case for SMA hysteresis behaviour, where strain in the first-order curves varies monotonically with stress.

Reviewing equations (18) and (19), given $z = F(\alpha, \beta)$, $\alpha = G_\alpha(z, \beta)$ can be defined as the inverse of $F(\alpha, \beta)$ with β fixed, or $\beta = G_\beta(\alpha, z)$ as the inverse with α fixed. Applying this to (21) and (22), the $u(t)$ required to produce a desired output $f(t)$ is obtained:

For an ascending branch

$$
u(t) = G_\alpha \left(\left[\frac{f(t) - f_{\min}}{2} - P_n \right], m_{n-1} \right) \tag{23}
$$

For a descending branch

$$
u(t) = G_\beta \left(M_n, \left[\frac{-f(t) + f_{\min}}{2} + P_n + F(M_n, m_{n-1}) \right] \right) \tag{24}
$$

where

$$
P_n = \sum_{k=1}^{n(t)-1} \left[F(M_k, m_{k-1}) - F(M_k, m_k) \right]
$$

5 EXAMPLES OF SMA

Based on the previous analysis, experiments have been carried out on Nitinol shape memory material to allow the modelling of the pseudoelasticity hysteresis. Through the explicit equations (18), (21) and (22), the weight function $\mu(\alpha, \beta)$ has been identified. The experiments have been compared with the model prediction within the SMA two-phase regions.

The test sample considered in this paper was an SMA Nitinol wire of 0.83 mm diameter and 200 mm length. Testing was limited to tension because the wires can only practically be tested in tension, so the relay output of elementary operators can be assumed only to take the values 0 and +1; the principle for the model calculation was the same as that used previously [22]. All of the tests were carried out at room temperature.

Figure 9 shows part of the collection of experimental first-order reversal curves used to compute the weight function $\mu(\alpha, \beta)$ for the Preisach model. The first-order transition curves are attached to the limiting ascending branch. Each of these curves was obtained by increasing the input monotonically to a certain value from zero and decreasing it to zero again. By using the experimental data shown in Fig. 9, values of $F(\alpha, \beta)$ on an evenly spaced grid of 36α and 233β values have been obtained from numerical interpolation between these curves. A cubic spline interpolation algorithm on the evenly spaced grid enabled computation of $F(\alpha, \beta)$ at any point α, β within the grid using programs written in Matlab [23]. Figure 9 also shows that the first-order reversal curves reproduced the experimental results.
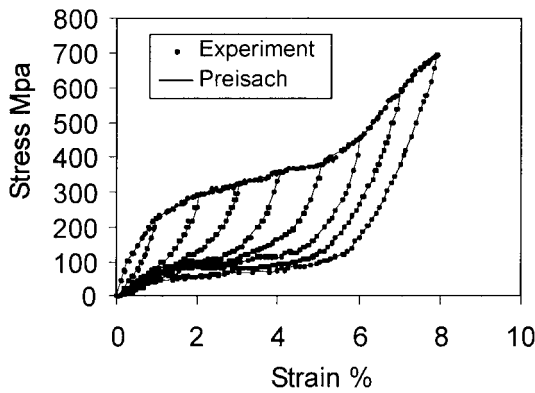
Fig. 9 First-order reversal curves for identification of $\mu(\alpha, \beta)$

Fig. 11 Internal hysteresis loop: comparison between experiment and model prediction

Based on the identified weight function $\mu(\alpha, \beta)$, a simulation model was constructed by using Matlab/Simulink. Only simple hysteresis relays were constructed in parallel, which establishes the effectiveness of the Preisach model as a mathematical model for memory.

Figure 10 illustrates the weight function identified from the first-order reversal curves. It is clear that the density of the weight function grid is different at different positions. Figure 11 is an example of the high-order transition curves predicted by the model. Minor loops 4–5–6 and 7–8–9 lie in the autensite/martensite two-phase region, where the wiping-out property can be seen clearly. The accuracy of the model can be affected by the density of the weight function and the different dissipation mechanisms between the forward and reverse phase transformation. The high-order internal curves are dependent on all the previous external curves through the return points, so errors will accumulate in the later internal curves, and therefore the error may be larger in the internal minor loop 7–8–9 than in minor loop 4–5–6.
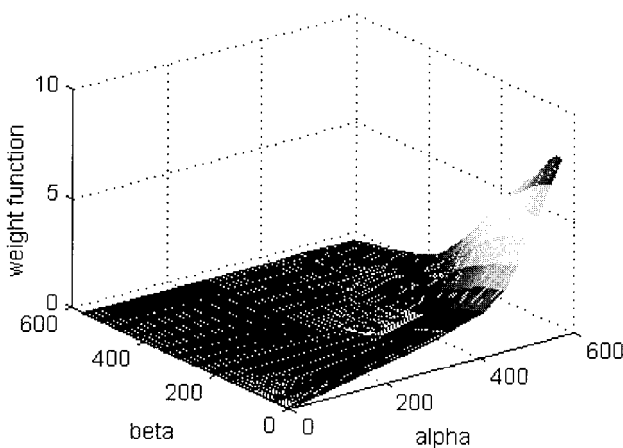
6 CONCLUSIONS

A distributed-element hysteresis model has been developed. This model is based on an approach that views the systems as consisting of a series of elementary hysteresis elements. As such, the model is consistent with the physical system.

Efficient and convenient equations based on the Preisach model have been obtained for the modelling of the input–output hysteresis behaviour. Simple identification and numerical implementation algorithms have been used to predict the response of the complex hysteresis system, based only on the first-order reversal transition curves. The present distributed-element model has been used for the analysis of hysteresis in SMA NiTi. The stress–strain curves followed by an NiTi wire under uniaxial tension have been investigated. At room temperature the alloy displays pseudoelasticity through martensite transformation, which results in the hysteretic effect.

The distributed-element hysteresis model can reproduce the essential features of the NiTi SMA transformation:

1. Inside the two-phase region the transformation curves depend on the previous inversion points, which the system can memorize.
2. The memory of the previous return points is wiped-out when the curve runs over the given point again.
3. If the input varies back-and-forth, the minor will be generated, and, between the same input extrema, the congruent minor loops can be generated.

The distributed-element Preisach model has been used satisfactorily to predict the hysteresis effect of SMAs. The higher-order transition curves are produced by using only first-order experimental data. In addition, since the model has a compact numerical form, it might find more applications for modelling other hysteresis materials.

Fig. 10 Weight function $\mu(\alpha, \beta)$

Through all these experiments and simulations, the hysteresis is assumed to be static and time plays no role other than as a parameter. Actually, the latent heat of transformation is exchanged between specimen and environment at a limited speed. The hysteretic effect of SMA has some relationship with the stress and strain rate. A modified Preisach model might be useful to model this rate-dependent effect [**24**].

ACKNOWLEDGEMENTS

REFERENCES

1 **Preisach F.** Uber die Magnetische Nachwirkung. *Zeitschrift für Physik*, 1935, **94**, 277–302.

2 **Brandon, J. A.** *Strategies for Structural Dynamic Modification*, 1990 (Research Studies Press, Chichester).

3 **Brandon, J. A.** Modal modelling of structures with isolated non-linearities. In *New Advances in Modal Synthesis of Large Structures* (Ed. L. Jezequel), 1997, pp. 447–456 (Balkema, Amsterdam).

4 **Krasnoselskii, M. A.** and **Pokrovskii, A. V.** *Systems with Hysteresis*, 1989 (Springer-Verlag, Heidelberg).

5 **Mayergoyz, I. D.** *Mathematical Models of Hysteresis*, 1991 (Springer-Verlag).

6 **Visintin, A.** *Differential Models of Hysteresis*, 1994 (Springer-Verlag).

7 **Brokate, M.** and **Sprekels, J.** *Hysteresis and Phase Transitions*, 1996 (Springer-Verlag, New York).

8 **Huo, Y. Z.** Preisach model for the hysteresis in shape memory alloys. In Proceedings of Plasticity '91, 3rd International Symposium on *Plasticity and Its Current Applications* (Eds J. P. Boehler and A. S. Khan), 1991, pp. 552–555 (Elsevier, London).

9 **Ortin, J.** Preisach modelling of hysteresis for a pseudo-elastic Cu–Zn–Al single crystal. *J. Appl. Phys.*, 1992, **71**(3), 1454–1461.

10 **Hughes, D.** and **Wen, J. T.** Preisach modelling of piezoceramic and shape memory alloy hysteresis. *Smart Mater.*

and Struct., 1997, **6**, 287–300.

11 **Iwan, W. D.** A distributed-element model for hysteresis and its steady dynamic response. *J. Appl. Mechanics*, December 1996, 893–900.

12 **Iwan, W. D.** The effective period and damping of a class of hysteretic structures. *Earthquake Engng and Struct. Dynamics*, 1979, **7**, 199–211.

13 **Iwan, W. D.** A model for system identification of degrading structures. *Earthquake Engng and Struct. Dynamics*, 1986, **14**, 877–890.

14 **Cifuentes, A. O.** and **Iwan, W. D.** Non-linear system identification based on modelling of restoring force behaviour. *Soil Dynamics and Earthquake Engng*, 1989, **8**(1), 2–8.

15 **Timoshenko, S. P.** *Strength of Materials*. Part 2. *Advanced Theory and Problems*, 1931, pp. 679–680 (New York).

16 **Graesser, E. J.** Multi-dimensional modelling of hysteretic materials including shape memory alloys: theory and experiment. PhD thesis, State University of New York at Buffalo.

17 **Sun, Q. P.** and **Hwang, K. C.** Micromechanics modelling for the constitutive behaviour of polycrystalline shape memory alloys—I: derivation of general relations. *J. Mechanics and Physics of Solids*, 1993, **41**(1), 1–17.

18 **Birman, V.** Review of mechanics of shape memory alloys structures. *Appl. Mechanics Rev.*, 1997, **50**(11), Part 1, 629–645.

19 **Brinson, L. C.** and **Huang, S.** Simplifications and comparisons of shape memory alloys constitutive models. *J. Intell. Mater. Syst. and Struct.*, January 1996, **7**, 108–118.

20 **Matsuzaki, Y.** Smart structures research in Japan. *Smart Mater. and Struct.*, 1997, **6**, R1–R10.

21 **Humbeeck, J. V.** and **Stalmans, R.** On the stability of shape memory alloys. In *Engineering Aspects of Shape Memory Alloys* (Eds T. W. Duerig *et al.*), 1990, pp. 96–105 (Butterworth-Heinemann).

22 **Song, C. L.** and **Brandon, J. A.** Estimation of local hysteretic properties for pseudo-elastic materials. In Proceedings of 2nd International Conference on *Identification in Engineering Systems*, Swansea, March 1999, pp. 210–219.

23 *Matlab: The Language of Technical Computing*, 1996 (The MathWorks Inc., Natick, Massachusetts).

24 **Dirk, A. P.**, **Luc, R.** and **Jan A. A. M.** Magneto-dynamic field computation using a rate-dependent Preisach model. In 6th MMM-INTERMAC Conference, Albupupu, New York, 1994.

C01300   © IMechE 2001